International Journal of Pavement Research and Technology
https://doi.org/10.1007/s42947-025-00523-6

社團法人中華鋪面工程學會
Chinese Society of Pavement Engineering

TECHNICAL NOTE

Diagnosis of Low-Carbon Permeable Pavements: Bearing Capacity and Long-Term Clogging Behaviour

Kiran Tota-Maharaj[1] · Sachini Shashiprabha Madushani[2] · John Monrose[3] · Upaka Rathnayake[4]

Received: 4 April 2024 / Revised: 11 September 2024 / Accepted: 8 February 2025

Abstract

The need to encourage sustainable construction practices to conserve the rapidly diminishing natural resources increases. Moreover, increases in impermeable areas in urban regions increase flood risk and impose significant stresses on stakeholders. The research presented here was conducted on using recycled low-carbon materials in permeable pavement systems (PPS) to address this issue. Despite the worldwide usage of PPS, uncertainty and a knowledge gap remain regarding the impact of recycled materials on their structural and long-term clogging performance. To this end, the load-bearing capacity and long-term clogging behaviour of four 0.2 m^2 permeable pavement rigs made up of varying natural and recycled sub-base materials were evaluated in the laboratory. The recycled materials selected were crushed concrete aggregates (CCA) and cement-bounded expanded polystyrene beads (C-EPS), and the natural materials were basalt and quartzite aggregates. Accelerated 10-year clogging simulation with yearly hydraulic conductivity measurements was used to evaluate the long-term clogging behaviour of the rigs, whilst portable falling weight deflectometer (PFWD) testing was used to evaluate the load-bearing capacity. The results of the clogging simulation found that the hydraulic conductivity of all rigs declined exponentially and were of a similar pattern. This confirmed that the sub-base materials had little influence on the clogging behaviour of permeable pavements. The PFWD test, however, demonstrated that the sub-base materials impacted the load-bearing capacity of the rigs, but both CCA and C-EPS were suitable to be used in permeable pavements under different loading restrictions.

Keywords Clogging · Crushed concrete aggregates · Expanded polystyrene · Permeable pavement · Portable falling weight deflectometer · Recycled construction materials

Abbreviations

PPS	Permeable pavement systems
CCA	Crushed concrete aggregates
C-EPS	Cement-bounded expanded polystyrene beads
PFWD	Portable Falling Weight Deflectometer
PICP	Permeable Interlocking Concrete Pavers
PSD	Particle Size Distribution
FWD	Falling Weight Deflectometer
LWD	Lightweight Deflectometer
CB	Crushed Brick
RCA	Recycled Concrete Aggregates
CDW	Construction and Demolition Waste
MSW	Municipal Solid Waste
AST	Accelerated Simulation Technique
G_s	Specific gravity
AIV	Aggregate Impact Value
MARV	Minimum Average Roll Value
LLGs	Limited-life Geotextiles
SS	Suspended Sediment
C_u	Coefficient of uniformity
C_c	Coefficient of curvature
k	Hydraulic conductivity

✉ Upaka Rathnayake
upaka.rathnayake@atu.ie

Kiran Tota-Maharaj
Kiran.Tota-Maharaj@rau.ac.uk

Sachini Shashiprabha Madushani
madushanijpss.23@uom.lk

John Monrose
John.Monrose@aecom.com

1 Royal Agricultural University (RAU) Cirencester, Gloucestershire GL7 6JS, England, UK

2 Department of Civil Engineering, University of Moratuwa, Moratuwa, Sri Lanka

3 AECOM, San Fernando, Trinidad and Tobago

4 Department of Civil Engineering and Construction, Faculty of Engineering and Design, Atlantic Technological University, Sligo, Ireland

Published online: 12 March 2025

1 Introduction

Permeable Pavement Systems (PPS) are engineered to perform dual functions as structural pavements and source control for stormwater [1]. They are pavements with structural requirements typically designed to satisfy lightly trafficked surfaces such as parking lots and pedestrian access whilst promoting infiltration and stormwater runoff mitigation [2–4]. This is significant in reducing peak flows and runoff volumes, improving stormwater runoff quality, and encouraging groundwater recharge where permitted. PPS supersede conventional paving with an at-source control to prevent or significantly delay stormwater runoff generation [1]. The typical structure consists of a permeable paving surface and layers of coarse aggregate materials that function as a storage reservoir during rainfall events [5]. Aggregates such as crushed stone are the most dominant component in PPS. Clean, single-sized or open-graded and angular aggregates are typically used for improved hydraulic and structural performance. The open voids between particles allow extremely high permeability, usually in excess of 25 m/h [5].

Numerous studies have commended PPS [6–10] for trapping sediments and other pollutants during the infiltration of stormwater runoff. However, this process can result in the clogging of the pavement surface, leading to reduced infiltration rates [11–13]. There is a perception that a conflict of interest makes others question the appropriateness of the word 'sustainable' for permeable pavement [14]. All infrastructure, including permeable pavements require maintenance [15]. Nevertheless, as with all filtration systems, permeable pavements will require the removal of trapped solids over time. Some studies [16–18] have found that for permeable pavements made up of Permeable Interlocking Concrete Pavers (PICP), fine particles accumulate in the upper layer of the pavement joints. Finer particles trap larger particles, resulting in increases in the rate of clogging [19]. Nicols and Lucke [20] found that Particle Size Distribution (PSD) curves could not be used as a stand-alone tool to infer PICP clogging processes but found that fine particles of sizes 251 to 550 µm contributed to lower infiltration rate measurements. Charlesworth et al. [10] found that after three years of monitoring, most of the sediments were in the surface layer of a porous asphalt laboratory test rig.

Numerous researchers [11–13] have shown an exponential decay of surface infiltration rate as a function of the age of the permeable pavement. Emerson et al. [21] reported that infiltration rates of permeable pavers were reduced by one to two orders of magnitude after three years of operation. Borgwardt [17] reported that the infiltration performance of permeable pavements decreases in the order of the power of ten after a few years of operation. Categories of PICP pavement clogging and associated infiltration rates are given in Lucke et al. [22]. These values could be used by engineers as a guide to assess clogging.

The majority of the literature on permeable pavements has focused on their role as a stormwater management tool, while the structural assessment of permeable pavement has received less attention [23]. The structural performance of permeable pavements consisting of interlocking concrete blocks is influenced by different variables such as surface block shape, depth, laying patterns, size and orientation of jointing and interconnection in addition to the quality of the base and sub-base reservoir materials [24, 25]. The Falling Weight Deflectometer (FWD) and Portable Falling Weight Deflectometer (PFWD), otherwise referred to as Lightweight Deflectometer (LWD), are often used in the field as dynamic non-destructive testing equipment to obtain the load–deflection response of pavement systems subjected to impulse loading [26, 27]. The PFWD provides quick and direct measurement of a near-surface, composite modulus parameter. The mechanism of the PFWD has been well presented by Kim et al. [28] and Fleming et al. [29]. The PFWD generates a force using a falling weight to create a deflection in the pavement equivalent to a moving vehicle with an axle load of approximately 1800 kg (4000 lbs) [25].

There is limited information on the use of deflectometer-type devices for the evaluation of the structural integrity of permeable pavements [23, 25, 26, 30]. Vancura et al. [23] used the FWD on pervious concrete in Minnesota to examine whether the empirical components of existing pavement analysis and design tools needed to be calibrated for pervious concrete separately from conventional concrete pavement. The authors compared the FWD deflection profiles of the pervious concrete pavements to those generated by the computer software ISLAB2005. Suleiman et al. [26] used the FWD on a pervious concrete pavement at Iowa State University, USA, with a 450 mm aggregate base and reported smaller deflections and better uniform support than traditional concrete pavement. A research team from the Toronto and Region Conservation [25] used a PFWD to test the stiffness of a PICP section of a parking lot at the Seneca College's King Campus a few kilometres north of Toronto, Canada. They reported that the PICP exhibited seasonal changes in strength, with the winter period accounting for the highest elastic modulus values and lowest deflection values. The researchers based this finding on the pavements being stiffer and more structurally sound during the winter when the upper base layers are frozen. When compared to asphalt pavement, the researchers found insignificant differences in strength. Henderson [30] used the PFWD to monitor the changes in the structural condition of five pervious concrete pavement sites and reported differences in the structural capacity of the pavements over the monitoring period.

Sustainable development should promote environmental preservation and conservation of the rapidly diminishing natural resources [31]. PPS are typically designed and constructed using large quantities of quarried construction aggregates. Such volumes of construction materials may not always be available when required. Intending to promote the sustainable use of natural materials, several countries, regions and municipalities across the world are accelerating their efforts towards formulating policies that promote the wide-scale recycling of waste products [32]. Advancement in infrastructural development provides significant opportunities for the use of waste and recycled materials, encouraging reduced waste disposal at landfills and/or environmental costs [32–34].

Numerous studies [35–38] have highlighted uncertainty and a knowledge gap regarding the performance of PPS, which consists of recycled materials. Whilst several researchers [39–44] have reported on the incorporation of recycled waste materials in permeable pavement concrete and asphalt surfaces, only a handful of studies [36, 45, 46] have reported on incorporating recycled materials as sub-base aggregates in permeable pavements. Moreover, each of these studies considered very limited performance evaluations. Rahman et al. [36] reported that Crushed Brick (CB) and Recycled Concrete Aggregates (RCA) from Construction and Demolition Waste (CDW) were suitable for use as sub-base materials in permeable pavements, but in evaluation, only geotechnical and hydraulic performances are considered. Rodriguez-Hernandez et al. [46] reported that Recycled Aggregates (RA) from CDW as sub-base materials in permeable pavements improved the hydrological output of the permeable pavements in terms of attenuation, retained rainfall, peak outflow and time to peak. Sañudo-Fontaneda et al. [45] used basic oxygen furnace slag as sub-base materials in permeable pavements but only evaluated the water quality infiltration performance of the pavements.

This paper encourages the use of recycled and low-carbon materials as sub-base materials in permeable pavements, producing new and original results and an analysis of the structural integrity and long-term clogging behaviour of permeable pavements consisting of new/different recycled materials. The use of recycled materials presents opportunities for the conservation of rapidly diminishing natural rocks, significantly reduces the carbon footprint during the production phase of pavements and promotes an ecologically sustainable solution to assist in managing Municipal Solid Waste (MSW). Specifically, two (2) recycled/recyclable materials, namely, Crushed Concrete Aggregates (CCA) and Cement-bounded Expanded Polystyrene beads (C-EPS), were used to compare against traditionally used natural materials (crushed basalt and quartzite aggregates) in the laboratory.

CCA are potential construction aggregates that have been produced in the laboratory from the crushing of aged precast units [47]. CCA consists of a stiff crushed aggregate core encapsulated by a relatively weak layer of mortar [48]. The crushed material has undergone a selective screening process, eliminating any undesirable material based on gradation requirements. Minimal information is available regarding the use of CCA in permeable pavements. Bentarzi et al. [49], in a laboratory study, mixed CCA with compost in a permeable pavement to increase the retention of pollutants and stimulate biological treatment. They did not consider or evaluate the effect of clogging in their study. However, CCA has been utilised in other construction applications, such as stone columns [50] and backfill material for pipe structures [48].

C-EPS is a novel, low-strength porous material produced in the laboratory. The primary constituents are cement and EPS beads. EPS beads can be regarded as a type of artificial, lightweight, low-density (less than 30 kg/m^3) non-absorbent aggregate. In construction, they can be used to produce lightweight, low-density concretes for building applications such as curtain walls, cladding panels, and composite flooring systems [51]. Expanded Polystyrene (EPS) is usually deemed an environmental menace because it is not biodegradable. However, it can easily be recycled into a product that can be utilised in practical sustainable construction. The common characteristics, handling, and uses of EPS have been discussed in detail by Mwasha et al. [52].

The use of CCA in permeable pavement construction lowers carbon emissions predominantly by reducing the demand for virgin aggregate and avoiding the energy-intensive processes involved in producing new materials. Moreover, concrete production is known to be a significant source of CO_2 emissions due to cement. Therefore, replacing virgin aggregates with CCA will reduce the embodied carbon of the pavement material [53–55]. Additionally, the use of EPS in concrete mixes helps to lower the overall weight and density of the pavement, which can lead to material efficiency through fewer emissions from production and transport. Further, C-EPS can enhance the insulating properties of the pavement, which may improve thermal regulation and reduce urban heat island effects [56].

The study revealed significant reductions in GHG emissions when CCA was incorporated, with reductions reaching up to 40% in some scenarios depending on transport distances and mixing ratios [54]. Another study estimates around 30–60% GHG reductions when recycled aggregates replace virgin materials [56].

The testing methods used significantly affect variations in the hydraulic properties of PPS. This research used the Accelerated Simulation Technique (AST) to simulate the clogging of four (4) permeable pavement rigs over ten years. Pratt [57] pioneered accelerated rainfall and sediment accumulation application techniques on laboratory-based PICP models. Numerous researchers [17, 18, 58–61] have since used AST along with hydraulic conductivity measurements for assessing the clogging patterns of laboratory-scale permeable pavements. These studies used a variety of sediment types, including natural and silica-based sediment. This study used natural sediment and tap water to replicate polluted stormwater. The PFWD test was used to evaluate the surface modulus (stiffness) and deflection profiles of the permeable pavement rigs in the laboratory.

2 Methods and Materials

2.1 Physical Testing of Aggregates

Particle Size Distribution (PSD) or gradation of the aggregates was determined by sieve analysis in accordance with ASTM-C136 [62] using a Humboldt "Mary Ann" Laboratory Sieve Sifter and 300 mm sieves. Aggregates were prepared to meet ASTM classifications No. 5, 57, and 8 for the sub-base, base and bedding layers respectively. These classifications are typically used in permeable pavements [63]. Specific gravity (G_s) and water absorption tests on the coarse aggregates were performed according to ASTM-C127 [64]. Bulk density (γ) and voids in course aggregate were conducted in accordance with ASTM-C29 [65]. The dry-rodded method of testing was used. Los Angeles (L.A) abrasion test was conducted according to ASTM-C131 [66]. This test is commonly used to indicate aggregate toughness and abrasion characteristics. The Aggregate Impact Value (AIV) test was carried out to evaluate the resistance to deterioration after the impact of aggregates. AIV was determined according to BS-812 [67]. The flakiness characteristics of the samples were determined according to BS-EN-933-3 [68]. pH values were determined in accordance with BS 1377 [69]. This method gives a direct reading of the pH value of a soil suspension in water.

The distribution is considered well-graded when Cu ranges between 4 and 6As expected, the specific gravity of the CCA fell at the low end of the 6–14% range of acceptable water absorption values for recycled materials in civil engineering applications [71]. The CCA performed well under the LA abrasion and impact tests with better results than the quartzite aggregates and below 50%. Notably, a significant portion of the abrasion was due to the cementitious paste (mortar) disintegration, which surrounded the natural aggregates. The pH of the CCA was notable, being significantly higher than the basalt and quartzite aggregates. This high pH value indicates high alkalinity, which can be attributed to the chemical composition of the cementitious paste, which is rich in $Ca(OH)_2$ and other oxides of alkaline elements. Based on these physical characteristics, CCA demonstrated potential as a suitable construction material to substitute or add to traditional quarried materials in permeable pavement applications.

2.2 Laboratory Setup

2.2.1 Design and Construction of Permeable Pavement Rigs

Four 450 × 420 × 610 (in mm) permeable pavement rigs were designed and constructed as tanked systems for testing in the laboratory. The rigs were made up of an 80 mm deep I-Paver interlocking concrete block surface with 2 to 13 mm joint spaces, a 50 mm deep bedding layer, a 100 mm deep base course and a 250 mm deep sub-base layer. Each block paver unit measured 80 × 197 × 143 (in mm) and weighed 4.35 kg. The sub-base layer was made up of different materials in each rig. Rig 1 contained basalt, Rig 2 quartzite, Rig 3 crushed concrete aggregates and Rig 4 C-EPS. Rig 4 contained a layer of Biaxial geogrid between the C-EPS block and the base course aggregates.

A nonwoven geotextile layer was placed between the bedding and aggregate base course layers for all rigs. The properties of the geotextile layer are listed in Table 1.

The Minimum Average Roll Value (MARV), as defined in ASTM D4433 [72], is a manufacturing quality control tool that provides users with a 97.7% degree of confidence that any samples will exceed reported values. Numerous researchers have reported on the ability of geotextiles to improve short-term pollutant removal efficiency [36, 73] as well as improving infiltration and attenuation of stormwater [74]. Mwasha [75] as well as Mwasha and Petersen [76] have recommended the use of limited-life Geotextiles (LLGs) for long-term geotechnical applications. However, these authors did not discuss the potential for using these geotextiles for short-term pollution removal.

Table 1 Mechanical and hydraulic properties of nonwoven geotextile

Property	Test method	MARV
Mechanical properties		
Grab tensile strength (N)	ASTM D4632	912
Trapezoid tear strength (N)	ASTM D4533	356
CBR puncture strength (N)	ASTM D6241	2224
Hydraulic properties		
Apparent opening size (mm)	ASTM D4751	0.18
Permittivity (s^{-1})	ASTM D4491	1.4
Flow rate ($l/min/m^2$)	ASTM D4491	3870
UV resistance after 500 h (% strength)	ASTM D4355	70

A commercially available biaxial geogrid with an ultimate tensile strength of 19.2 kN/m was placed between the C-EPS block and the aggregate base course layer in Rig 4. The purpose of the geogrid was to reinforce the pavement and to reduce the load transferred to the C-EPS block. The physical and mechanical properties of the geogrid are listed in Table 2.

2.2.2 Stormwater Delivery System

A purpose-built Rainfall Simulation Infiltrometer (RSI), designed and built from guidance from the literature [77], was used to deliver semi-synthetic stormwater to the rigs.

Table 2 Physical and mechanical properties of the biaxial geogrid

Property	Value
Aperture dimensions (mm)	25
Minimum rib thickness (mm)	1.27
Tensile strength @ 2% Strain (kN/m)	6.0
Tensile strength @ 5% Strain (kN/m)	11.8
Ultimate tensile strength (kN/m)	19.2
Junction efficiency (%)	93
Flexural stiffness (mg-cm)	750,000
Aperture stability (m-N/deg)	0.65

Numerous studies [78–81] have successfully used rainfall simulation techniques for practical research in urban drainage. The experimental setup is shown in Fig. 1. It consisted of a 100 L mixing tank equipped with a submersible pump and a Stir-Pak variable-speed heavy-duty mixer, valves to control flow rates, flow meters to measure flow rates, and a stormwater distributor arm made of perforated PVC pipes. The mixer ensured the sediment loading remained in homogenous suspension during the experiments.

2.3 Experimental Procedure

2.3.1 Hydraulic Conductivity and Long-Term clogging

Semi-synthetic stormwater comprised of tap water and fine sediments (300 µm in diameter) and tap water was used as the clogging agent. The fine sediments were sourced from a local quarry. The PSD curve of the sediments is shown in Fig. 2. The purpose-built RSI was used to supply the semi-synthetic stormwater to the rigs. The fine sediments were chosen because numerous studies [19, 20] have reported that finer materials contribute disproportionally to accelerated clogging of permeable pavements.

The clogging pattern of the permeable pavement rigs was determined from yearly hydraulic conductivity measurements over an accelerated 10-year period. This assumes

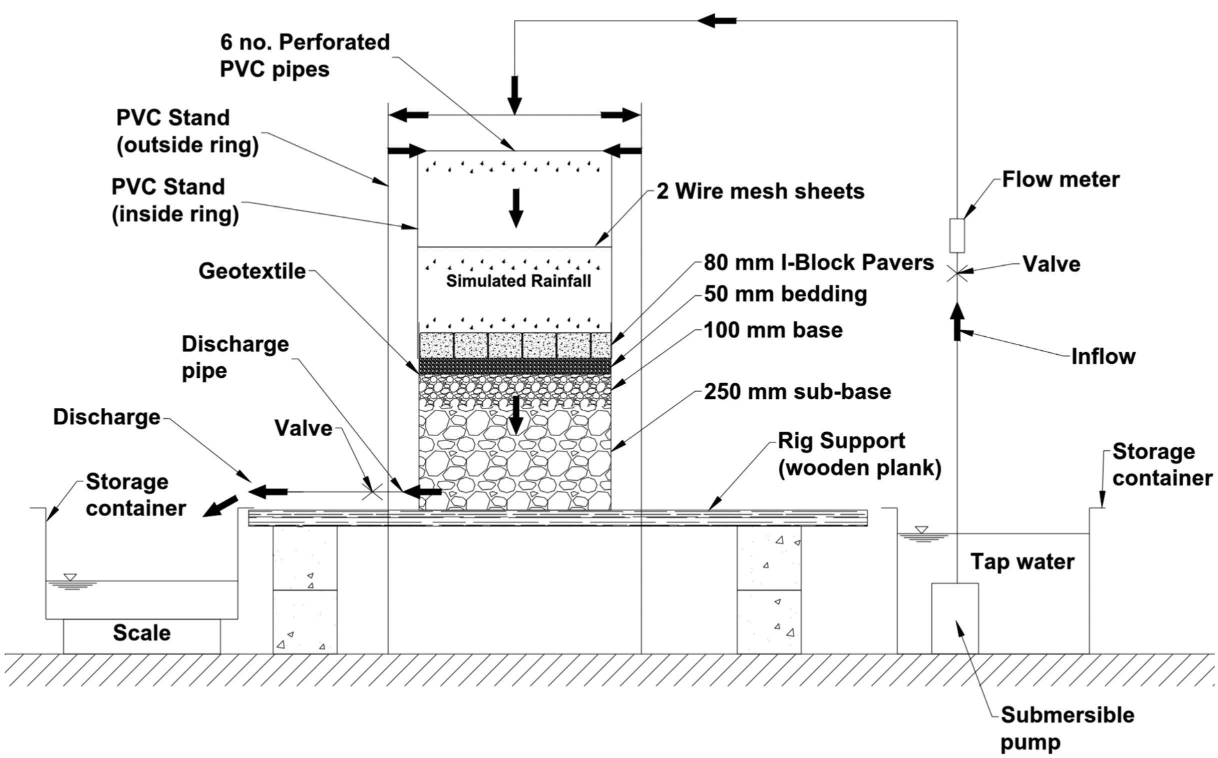

Fig. 1 Permeable pavement laboratory setup

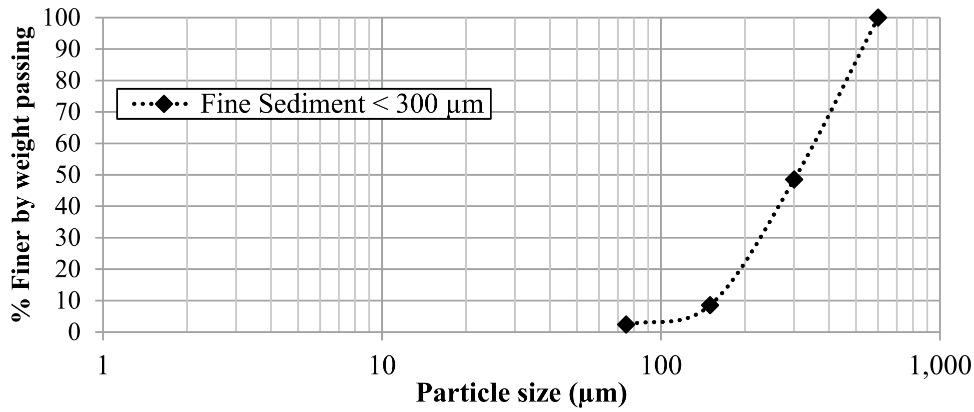

Fig. 2 PSD of the sediments used to clog the experimental rigs

that, in practice, most permeable pavement installations will receive additional sediment at every rainfall event. Inflow volumes into the permeable pavement test rigs were calculated from the product of the plan surface area (0.189 m^2) of the rigs and the yearly rainfall depth. The Caribbean region has an average annual rainfall depth of approximately 2000 mm [82]. Hence, with each rig having a surface area of 0.189 m^2, an inflow stormwater volume of 378 L was required to deliver the equivalent of one year's rainfall to the permeable pavement test rigs. This value was rounded up to 400 L for ease of measurement.

Based on literature [58, 60], an average Suspended Sediment (SS) loading of 200 mg/L or 80 g/400 L was used in this study. A falling head permeability test [83] was used to determine the hydraulic conductivity after each year. The coefficient of permeability was then calculated from Darcy's law as a falling head test [84]. A minimum 24-h drying period was set for each rig before performing the hydraulic conductivity tests. Variation in sediment accumulation from year 1 to year 10 of the accelerated clogging simulation of one of the rigs is shown in Fig. 3.

Statistical analyses of the results were performed using the IBM statistical computer software Statistical Package for the Social Sciences (SPSS) version 20 [85]. Pearson's correlations and regression models were done to test the hypothesis that the hydraulic conductivity of permeable pavements decreases over time because of clogging. A 95% confidence interval was used for all statistical analyses. The variables used in the regression models were hydraulic conductivity (dependent variable) and service life/age of permeable pavement (independent variable).

2.3.2 Load Bearing Capacity

Stiffness and deflection profiles of the permeable pavement rigs were assessed using a PRIMA 100 PFWD. PFWD is modelled after the FWD but uses a much lighter weight, making it portable and able to be manually operated. The relationship between load and deflection, created by the free-falling weight, is measured using the PFWD [28, 86]. The PRIMA 100 PFWD consisted of a 300 mm diameter base (loading) plate with a sensor and a falling weight (10 kg sliding hammer), which was dropped onto the plate from a height of 850 mm. The base incorporates two sensors: a load cell and a geophone (velocity transducer).

During testing, the load is applied to the surface of the rigs via the base plate. The resulting force and velocity/time histories are measured above and below the centre of the plate, respectively. The corresponding displacement/time history is automatically obtained via integration (internal to the device) of the velocity record. The output includes respective time histories and peak values of the applied load

Fig. 3 Accelerated clogging simulation example **a** Year 1, **b** Year 10

and ensuing deflection, as well as an estimated value of the surface modulus, E_0 [87]. E_0 is based on the Boussinesq solution relating the static deflection of an elastic half-space subjected to an axisymmetric surface loading [88].

All measurements were recorded, interpreted, calculated, and stored in a personal digital assistant (PDA) device connected to the PRIMA 100 device via a wireless Bluetooth connection. The deflections were measured at the centre of the loading plate. Six PFWD measurements were taken for each rig set-up. All measurements were performed under identical conditions for all rigs. The first two drops were excluded from analyses as they were considered seating. The remaining four were used for analysis and comparison.

A literature survey confirmed that PFWD testing of permeable pavements is uncommon and limited to field installations. Despite scarce literature sources on PFWD testing of permeable pavements, the methodology employed in this paper, utilising the PRIMA 100 PFWD, was practical for evaluating and comparing the bearing capacity (stiffness and deflection) of the pavement rigs in the laboratory.

3 Results and Discussion

3.1 Particle Size Distribution of the Selected Aggregates

PSD or gradation curves of the unbound aggregates used in each rig are shown in Fig. 4. The bedding course, base course, and sub-base aggregates were graded to satisfy ASTM classifications Nos. 8, 57, and 5, respectively.

Based on the gradation curves, the coefficient of uniformity (C_u) and coefficient of curvature (C_c) values were calculated [70]. The distribution is considered well-graded when C_u ranges between 4 and 6. Conversely, when C_u is less than 4, the distribution is considered poorly or uniformly graded. The presented results show that the distribution of all aggregates was uniformly graded ($C_u < 4$).

Table 3 presents the physical characteristics of the aggregates used. The CCA's specific gravity was, as expected, lower than that of basalt and quartzite aggregates but greater than the typical requirement of 2.0 kg/m3 [36]. Conversely, the CCA's water absorption was significantly higher than that of basalt and quartzite aggregates but less than the typical requirement of 10% [36].

3.2 Hydraulic Conductivity and Long-Term Clogging

The infiltration capacities and clogging pattern of the permeable pavement rigs based on calculated hydraulic conductivity changes after ten years of accelerated simulation of semi-synthetic stormwater made up of tap water and fine sediment are shown in Table and Fig. 5. Hydraulic conductivities were predictably high at the commencement of the tests, considering that the rigs were constructed with joints (2–13 mm) containing ASTM No.8 bedding stone. The values presented in Table 4 and graphs shown in Fig. 5 show a decline in hydraulic conductivity as a function of service life (clogging) of the permeable pavement rigs. Hydraulic

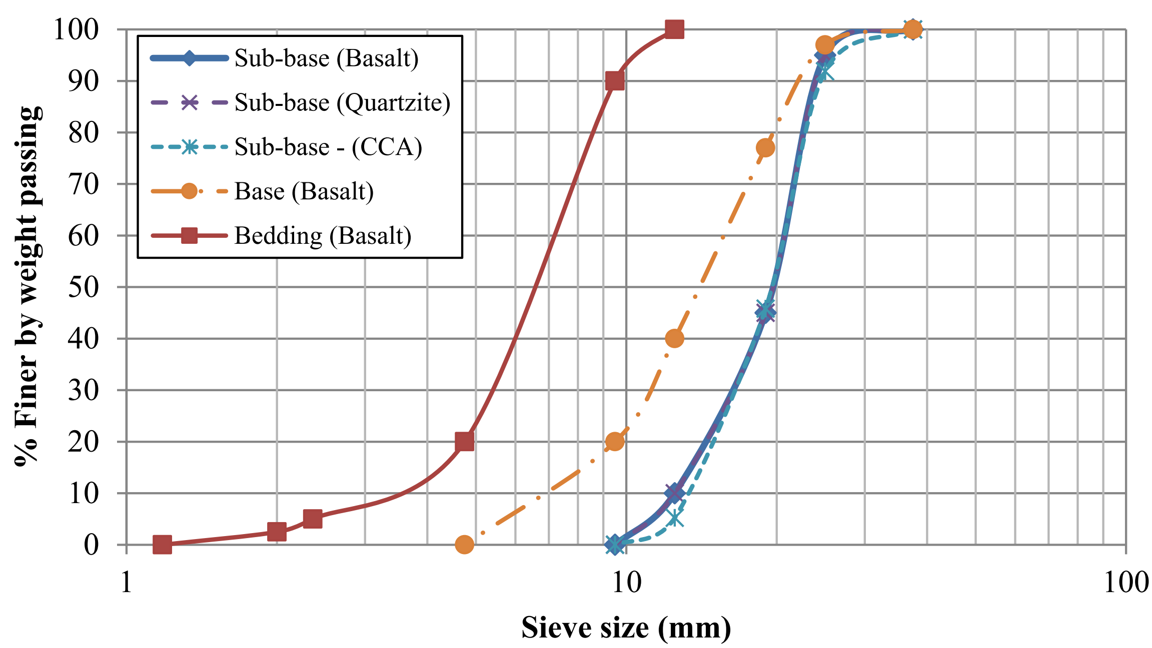

Fig. 4 Particle size distributions (PSD) of unbound pavement aggregates

Table 3 Physical properties of unbound aggregates

Properties	Bedding	Base	Sub-base		
			Rig 1—Basalt	Rig 2—Quartzite	Rig 3—CCA
ASTM grading classification	No. 8	No. 57	No. 5	No. 5	No. 5
Coefficient of uniformity (C_u)	2.3	2.5	1.6	1.6	1.5
Coefficient of curvature (C_c)	1.3	1.1	0.8	0.8	0.9
Specific gravity, G_s (kg/m^3)	2.709	2.709	2.709	2.575	2.245
Water absorption (%)	1.2	1.2	1.2	0.8	7.1
L.A abrasion (%)	18	18	18	53	44
Impact (%)	16	16	16	38	42
Flakiness index (%)	1	1	1	3	-
Bulk density (kg/m^3)	1530	1559	1541	1504	1252
SSD bulk density (kg/m^3)	1548	1578	1559	1516	1341
Voids ratio, e	0.433	0.422	0.429	0.414	0.44
Porosity, n (%)	30	30	30	29	31
pH	8.51	8.51	8.51	8.28	12.26

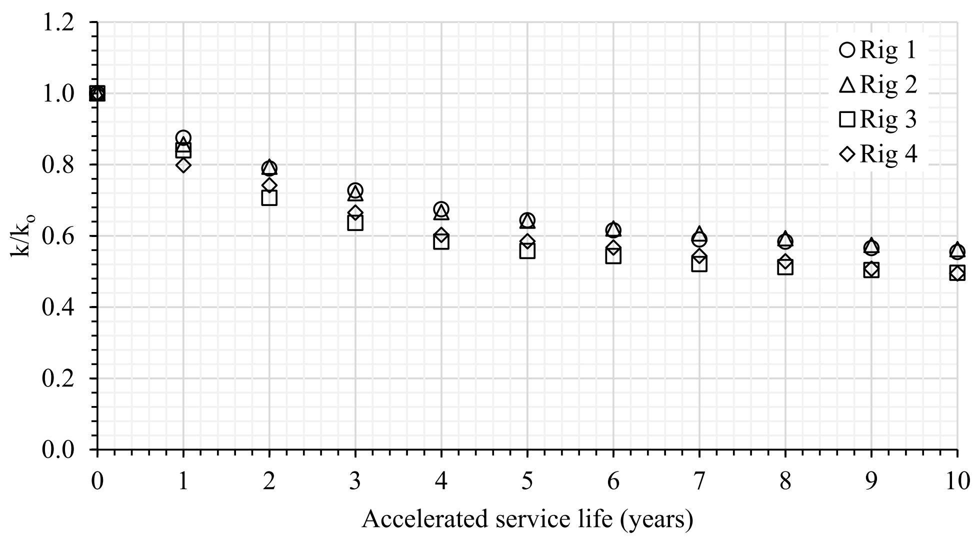

Fig. 5 Reduced hydraulic conductivity coefficients of the pavement rigs

Table 4 Hydraulic conductivity results of the pavement rigs

Year	Hydraulic conductivity, k (mm/h)			
	Rig 1	Rig 2	Rig 3	Rig 4
0	5780	5994	5138	4516
1	5057	5138	4316	3605
2	4559	4760	3630	3351
3	4204	4316	3269	3004
4	3900	3996	2997	2723
5	3720	3853	2864	2640
6	3557	3720	2790	2562
7	3407	3637	2675	2454
8	3372	3557	2631	2387
9	3269	3443	2589	2293
10	3205	3372	2549	2234

conductivities were reduced by 45%, 44%, 50% and 51% in Rig 1, Rig 2, Rig 3 and Rig 4, respectively. Greater reductions were not obtained over the 10-year accelerated period, most likely because some joints remained with relatively few sediment accumulations, and some sediments remained over the surface of the concrete block pavers rather than getting trapped within the joints between the pavers. This exponential decline in hydraulic conductivity reduction agrees with previous studies [11–13, 17].

Reductions in the rigs' hydraulic conductivities (refer to Fig. 6) were found to have a similar pattern and rate for all rigs. This observation was not surprising due to the similarity in the pavement structure of the rigs above the sub-base layer. The rigs were also subjected to the same clogging agent under similar rainfall application rates. Numerous

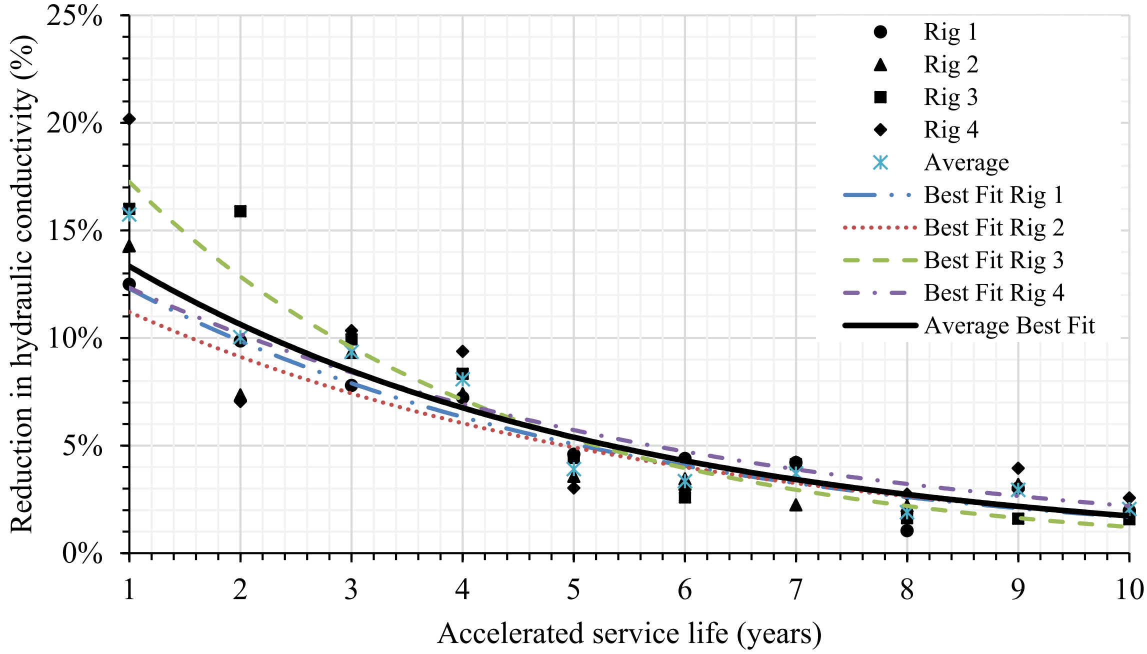

Fig. 6 Observed percent reduction in hydraulic conductivities of the pavement rigs

Table 5 Pearson's correlation coefficients for hydraulic conductivity and service life of each pavement rig

		Hydraulic conductivity, k				Year
		Rig 1	Rig 2	Rig 3	Rig 4	
Year	Pearson correlation	−0.931	−0.920	−0.880	−0.905	1
	Sig. (2-tailed)	0	0	0.001	0.001	

studies [16–18] have found that fine particles accumulate in the upper layer of the pavement joints for PICPs, resulting in clogging. The variation in sub-base materials most likely had an insignificant influence on the hydraulic conductivities of the rigs.

3.2.1 Statistical Analysis

3.2.1.1 Correlation Analysis Pearson's correlation in SPSS was used to test the hypothesis that aged permeable pavements without maintenance have reduced hydraulic conductivities because of clogging. The results presented in Table 5, show that for all rigs, there is a significant ($p < 0.01$) negative correlation between hydraulic conductivity and service life (age) of the pavements. The correlations are also strong (0.88 to 0.93).

3.2.1.2 Regression Analysis The details of the regression models done in SPSS are presented in Table 6. Both linear and exponential regression models were analysed at a 95% confidence level. In all cases, the exponential regression model simulated a better fit of the observed values as indicated by the higher R^2 values, which ranged from 0.84 (Rig 3) to 0.91 (Rig 1). Graphical illustrations of the exponential regression models are shown in Fig. 7.

Table 6 Regression models for all permeable pavement rigs analysed under accelerated clogging simulations

Rig no.	Equation	Regression model	R^2
1	Linear	$k = -232.045A + 5162.955$	0.87
	Exponential	$k = 5191.810e^{-.056A}$	0.91
2	Linear	$k = -228.482A + 5304.773$	0.85
	Exponential	$k = 5323.052e^{-.052A}$	0.90
3	Linear	$k = -220.409A + 4324.591$	0.77
	Exponential	$k = 4313.997e^{-.064A}$	0.84
4	Linear	$k = -189.191A + 3834.045$	0.82
	Exponential	$k = 3846.884e^{-.062A}$	0.89

k = hydraulic conductivity; A = age (service life) of pavement based on accelerated clogging simulation

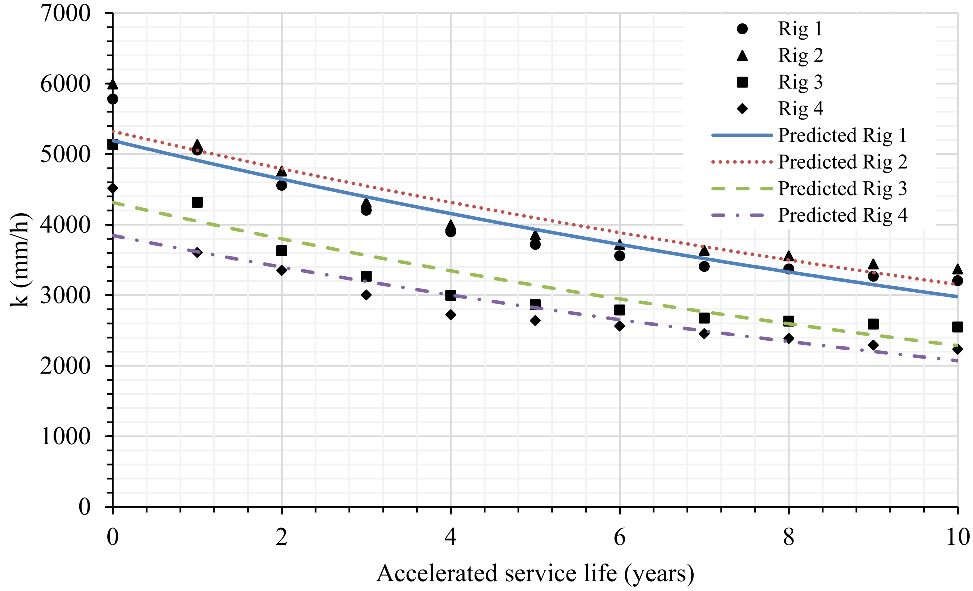

Fig. 7 Exponential regression model for the pavement rigs under laboratory accelerated clogging scenarios

3.3 Structural Performance

3.3.1 Load Bearing Capacity

Permeable pavements are typically designed for low-speed, low-volume traffic areas such as parking lots and pedestrian walkways. Despite this bearing capacity limitation, it is essential that permeable pavements remain structurally sound throughout their life cycle. This experiment evaluated and compared the bearing capacity (stiffness and deflection) of the pavement rigs in the laboratory using a PRIMA 100 PFWD. In general, the test involved dropping a 10 kg weight on the surface of the pavement rigs, and sensors measured the deflection and stiffness of the pavement at the centre of the loading. An example of PRIMA 100 PFWD on one of the rigs is shown in Fig. 8. It must be noted that the permeable pavement rigs were subjected to a series of water quality, hydrological and accelerated clogging tests prior to deflectometer testing. The rigs were not subjected to any additional loading other than that provided by the PFWD; hence, changes in the structural capacity of the rigs over time were not monitored and are outside the scope of this paper.

Bar graphs of the mean deflection and surface modulus results of the PFWD tests are shown in Fig. 9. The results were as expected, with Rig 1 recording the lowest mean deflection (493 μm) and the highest surface modulus (53 MPa), while Rig 4 recorded the highest deflection (1095 μm) and the lowest surface modulus (24 MPa).

The graphs presented in Figs. 10 and 11 show the profiles of the applied load and the deflection bowl respectively for the structural response of the rigs using the PRIMA 100 PFWD. It is noted that the peak values of the deflection signals for all rigs lag behind the respective

Fig. 8 PFWD testing on one pavement rig

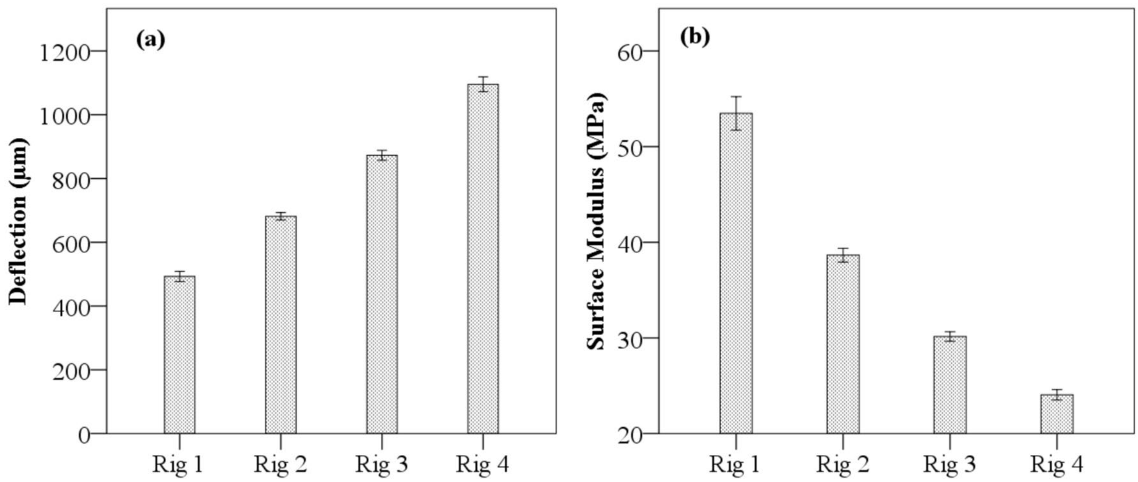

Fig. 9 Box plots of the mean deflection (**a**) and surface modulus (**b**) results from the four rigs

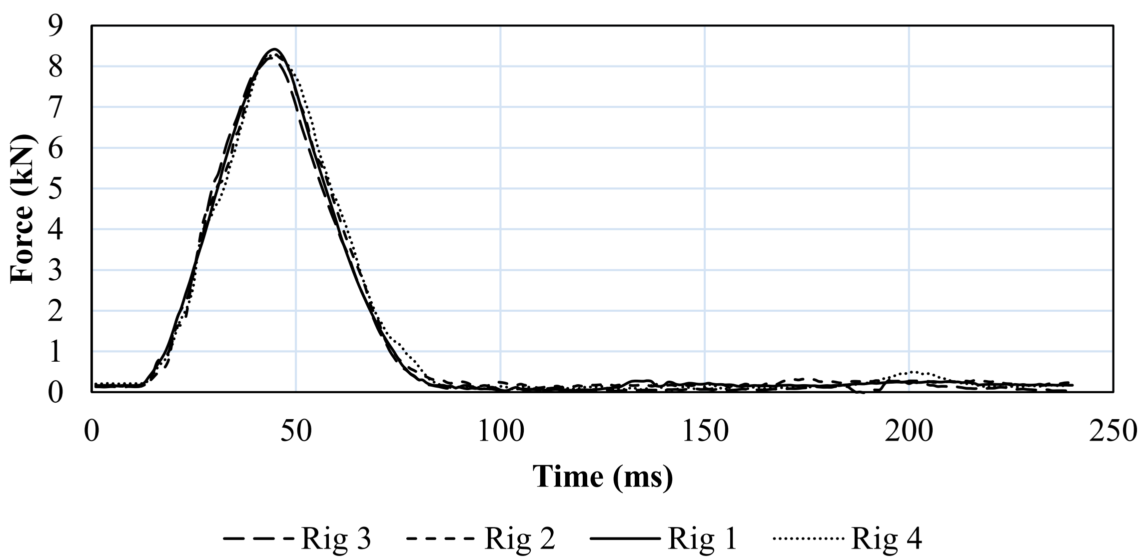

Fig. 10 Force signal response from the PRIMA 100 PFWD for each rig

peak forces. Some studies [29, 87] have reported this trend, which according to Hoffmann et al. [87] is due to the effects of inertia.

Figure 11 highlights a section of the deflection plots with large negative deflection values (in the cloud). Such response type indicates incomplete compaction or excessive moisture, which is characteristically expected for permeable pavements. The typical deflection response outputs from the PRIMA 100 PFWD are shown in Fig. 12.

Figure 13 illustrates the ISM values of the varying permeable pavement rigs. ISM values varied between rigs ranging from 7.5×10^{-3} kN/mm (Rig 4) to 17.1×10^{-3} kN/mm (Rig 1). Rigs 2 and 3 recorded $12.3 \times 10–3$ kN/mm values and 9.3×10^{-3} kN/mm respectively.

4 Conclusions

In this study, the hydraulic conductivity, permeability and long-term clogging patterns were assessed from the simulation of 10 years of accumulated natural sediment. Hydraulic conductivity measurements were made after each simulated year. The results show a decline in hydraulic conductivity as a function of the service life (clogging) of the permeable pavement rigs. Hydraulic conductivities were reduced by 45%, 44%, 50% and 51% in Rig 1, Rig 2, Rig 3 and Rig 4, respectively. Pearson's correlations, r and regression models were performed to test the hypothesis that the hydraulic conductivity of permeable pavements decreases over time

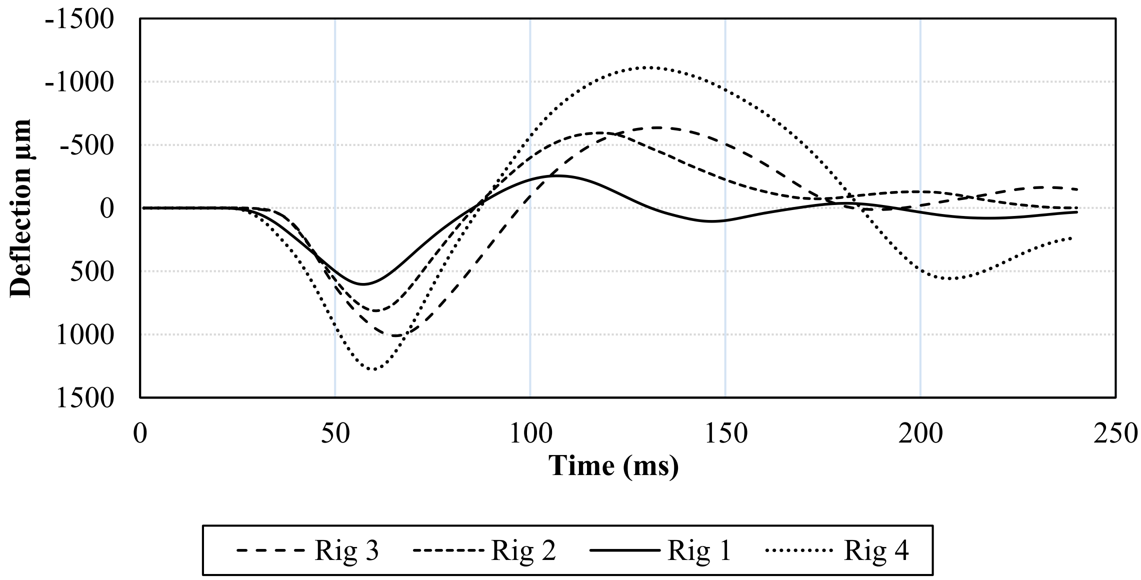

Fig. 11 Deflection response output from PRIMA 100 PFWD for each rig

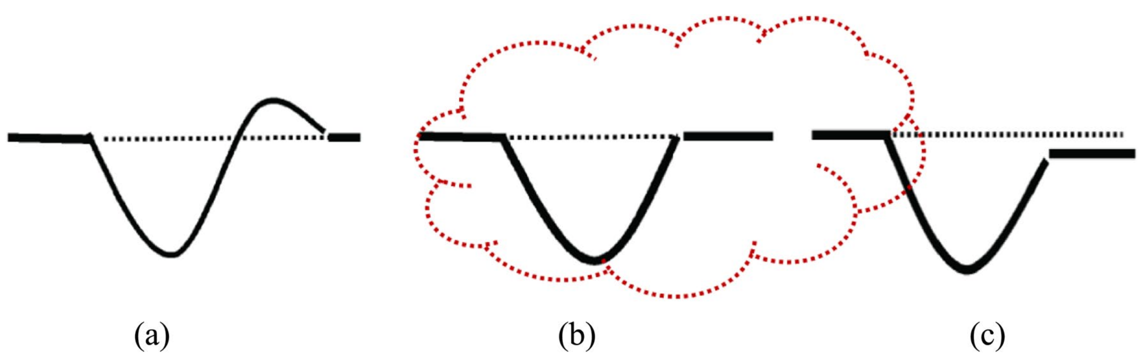

Fig. 12 Typical deflection responses from Prima 100 PFWD **a** incomplete compaction or excessive moisture, **b** ideal, **c** poor compaction [82]

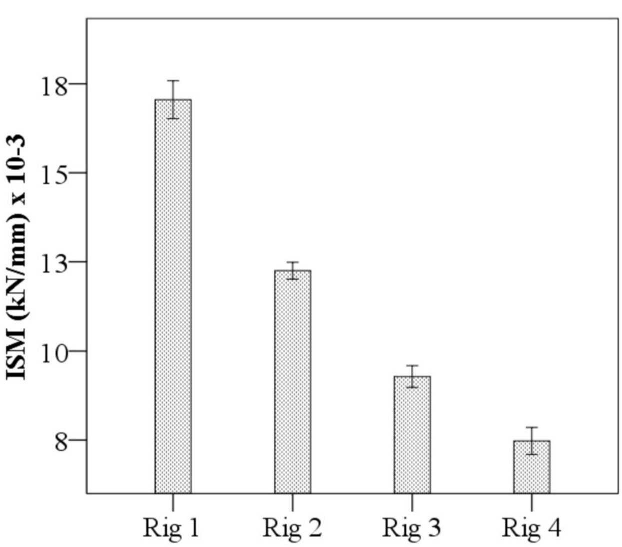

Fig. 13 Impact stiffness modulus of the permeable pavement rigs

because of clogging. The results of the Pearson's correlation, *r*, showed that for all rigs, there was a significant ($p < 0.01$) negative and strong correlation between hydraulic conductivity and service life (age) of the pavements. A comparison between linear and exponential regression models confirmed that the exponential regression models simulated a better fit of the observed values. The results were similar for all rigs, confirming that the sub-base component did not significantly affect the clogging pattern of the permeable pavement rigs. The results confirmed that the hydraulic conductivity of permeable pavements decreases exponentially over time because of clogging. Excessive reduction in hydraulic conductivity occurred within the first three years of simulated accumulation of sediments over the surface joints of the permeable pavement rigs. Therefore, it is recommended to perform restorative maintenance through sweeping, vacuuming or removal and replacement of surface joint material during this time period.

This study also addressed the load-bearing capacity (stiffness and deflection) of the pavement rigs, which was evaluated through Portable Falling Weight Deflectometer (PFWD) testing in the laboratory. All rigs behaved differently in terms of surface modulus and deflection. Rig 1 (basalt) recorded the lowest mean deflection (493 ± 10.1 μm) and the highest mean surface modulus (53 ± 1.1 MPa), whereas Rig 4 (C-EPS) recorded the highest mean deflection (1095 ± 14.6 μm) and the lowest mean surface modulus (24 ± 0.3 MPa). Rig 3 had mean deflection and surface modulus values of 873 ± 9.8 μm and 30 ± 0.3 MPa, respectively, whilst Rig 2 had mean deflection and surface modulus values of 681 ± 7.4 μm and 39 ± 0.5 MPa, respectively. The results of the PFWD testing have demonstrated that CCA and C-EPS can maintain the structural integrity of permeable pavements when used as sub-base materials. However, due to lower stiffness and higher deflection values obtained from Rig 4, which contained C-EPS, it is recommended that C-EPS be utilised as sub-base materials at locations that receive little to no vehicular traffic loads such as building aprons, pedestrian access, bicycle lanes, sidewalks etc. As a future recommendation, the authors suggest researching the potential for using limited-life geotextiles for short-term pollution removal. The authors further recommend that structural and clogging evaluations be conducted on field permeable pavements exposed to varying environmental and loading conditions.

Acknowledgements None.

Authors' Contributions KT conceptualized the research work and wrote the initial draft; SSM analysed the data and wrote the initial draft; JM conducted the experiments and gathered the data; UR conceptualized the research work and reviewed the paper.

Funding Open Access funding provided by the IReL Consortium. This research has not received funding from research bodies.

Availability of Data and Materials Data are available from the corresponding author by request.

Declarations

Conflict of interest The authors declare no conflicts of interest.

References

1. Fassman, E. A., & Blackbourn, S. (2010). Urban runoff mitigation by a permeable pavement system over impermeable soils. *Journal of Hydrologic Engineering, 15*(6), 475–485.
2. Scholz, M., & Grabowiecki, P. (2007). Review of permeable pavement systems. *Building and Environment, 42*(11), 3830–3836.
3. Jato-Espino, D., Sillanpää, N., Charlesworth, S., & Andrés-Doménech, I. J. W. (2016). Coupling GIS with stormwater modelling for the location prioritization and hydrological simulation of permeable pavements in urban catchments. *Water, 8*(10), 451.
4. Rodríguez-Rojas, M. I., Huertas-Fernández, F., Moreno, B., Martínez, G., & Grindlay, A. L. (2018). A study of the application of permeable pavements as a sustainable technique for the mitigation of soil sealing in cities: A case study in the south of Spain. *Journal of Environmental Management, 205*, 151–162.
5. Ferguson, B. K. (2005). *Porous pavements* (p. 600). CRC Press.
6. Brattebo, B. O., & Booth, D. B. (2003). Long-term stormwater quantity and quality performance of permeable pavement systems. *Water Research, 37*(18), 4369–4376.
7. Bean, E. Z., Hunt, W. F., & Bidelspach, D. A. (2007). Evaluation of four permeable pavement sites in Eastern North Carolina for runoff reduction and water quality impacts. *Journal of Irrigation and Drainage Engineering, 133*(6), 583–592.
8. Collins, K. A. (2007). *A field evaluation of four types of permeable pavement with respect to water quality improvement and flood control. Masters dissertation*. North Carolina State University.
9. Beecham, S., Pezzaniti, D., & Kandasamy, J. (2012). Stormwater treatment using permeable pavements. *Proceedings of the Institution of Civil Engineers—Water Management, 165*(3), 161–170.
10. Charlesworth, S. M., Beddow, J., & Nnadi, E. O. (2017). The fate of pollutants in porous asphalt pavements, laboratory experiments to investigate their potential to impact environmental health. *International Journal of Environmental Research and Public Health, 14*(6), 666.
11. Sansalone, J., Kuang, X., & Ranieri, V. (2008). Permeable pavement as a hydraulic and filtration interface for urban drainage. *Journal of Irrigation and Drainage Engineering, 134*(5), 666–674.
12. Permeable Pavements: Guide to the design, construction and maintenance of concrete block permeable pavements, 6th ed, Uniclass L534:L217, Interpave, Leicester, UK, 2010, pp. 1–80 (can be accessed via ku.gro.gnivap.www//:ptth).
13. Winston, R. J., Al-Rubaei, A. M., Blecken, G. T., Viklander, M., & Hunt, W. F. (2016). Maintenance measures for preservation and recovery of permeable pavement surface infiltration rate: The effects of street sweeping, vacuum cleaning, high pressure washing, and milling. *Journal of Environmental Management, 169*, 132–144.
14. Butler, D., & Davies, J. W. (2011). *Urban drainage* (3rd ed., pp. 543–544). Spon Press.
15. Sansalone, J., Kuang, X., Ying, G., & Ranieri, V. (2012). Filtration and clogging of permeable pavement loaded by urban drainage. *Water Research, 46*(20), 6763–6774.
16. Pratt, C. J., Mantle, J. D. G., & Schofield, P. A. (1995). UK research into the performance of permeable pavement, reservoir structures in controlling stormwater discharge quantity and quality. *Water Science and Technology, 32*(1), 63–69.
17. Borgwardt, S. (2006). Long-term in-situ infiltration performance of permeable concrete block pavement. In *8th international conference on concrete block paving, San Francisco, CA, USA*.
18. Siriwardene, N. R., Deletic, A., & Fletcher, T. D. (2007). Clogging of stormwater gravel infiltration systems and filters: Insights from a laboratory study. *Water Research, 41*(7), 1433–1440.

19. Balades, J. D., Legret, M., & Madiec, H. (1995). Permeable pavements: Pollution management tools. *Water Science and Technology, 32*(1), 49–56.
20. Nicols, P. W. B., & Lucke, T. (2017). A detailed analysis of sediment particle sizes and clogging in permeable pavements. *CLEAN – Soil Air Water, 45*(4), 170078.
21. Emerson, C. H., Wadzuk, B. M., & Traver, R. G. (2010). Hydraulic evolution and total suspended solids capture of an infiltration trench. *Hydrological Processes, 24*(8), 1008–1014.
22. Lucke, T., White, R., Nichols, P., & Borgwardt, S. (2015). A simple field test to evaluate the maintenance requirements of permeable interlocking concrete pavements. *Water, 7*(6), 2542–2554.
23. Vancura, M., Macdonald, K., & Khazanovich, L. (2011). Structural analysis of pervious concrete pavement. *Transportation Research Record: Journal of the Transportation Research Board, 2226*(1), 13–20.
24. Jamshidi, A., Kurumisawa, K., White, G., Nishizawa, T., Igarashi, T., Nawa, T., & Mao, J. (2019). State-of-the-art of interlocking concrete block pavement technology in Japan as a post-modern pavement. *Construction and Building Materials, 200*, 713–755.
25. Toronto and region conservation, performance evaluation of permeable pavement and a bioretention swale—Seneca College, King City, Ontario Toronto and Region Conservation Authority, Ontario, Canada (2008)
26. Suleiman, M. T., Gopalakrishnan, K., & Kevern, J. T. (2011). Structural response of pervious concrete pavement systems using falling weight deflectometer testing and analysis. *Journal of Transportation Engineering, 137*(12), 907–917.
27. Mallick, R. B., & El-Korchi, T. (2017). *Pavement engineering—principles and practice* (3rd ed., p. 663). CRC Press.
28. Kim, J. R., Kang, H. B., Kim, D., Park, D. S., & Kim, W. J. (2007). Evaluation of In situ modulus of compacted subgrades using portable falling weight deflectometer and plate-bearing load test. *Journal of Materials in Civil Engineering, 19*(6), 492–499.
29. Fleming, P. R., Frost, M. W., & Lambert, J. P. (2007). Review of lightweight deflectometer for routine in situ assessment of pavement material stiffness. *Transportation Research Record: Journal of the Transportation Research Board, 25*, 80–87.
30. Henderson, V. (2012). *Evaluation of the performance of pervious concrete pavement in the Canadian Climate. Doctoral thesis*. University of Waterloo.
31. Rao, A., Jha, K. N., & Misra, S. (2007). Use of aggregates from recycled construction and demolition waste in concrete. *Resources, Conservation and Recycling, 50*(1), 71–81.
32. Inyang, H. I. (2003). Framework for recycling of wastes in construction. *Journal of Environmental Engineering, 129*(10), 887–898.
33. Chang, N., Wang, H. P., Huang, W. L., & Lin, K. S. (1999). The assessment of reuse potential for municipal solid waste and refuse-derived fuel incineration ashes. *Resources, Conservation and Recycling, 25*(3–4), 255–270.
34. Behera, M., Bhattacharyya, S. K., Minocha, A. K., Deoliya, R., & Maiti, S. (2014). Recycled aggregate from C&D waste & its use in concrete—A breakthrough towards sustainability in construction sector: A review. *Construction and Building Materials, 68*, 501–516.
35. Weiss, P. T., Kayhanian, M., Gulliver, J. S., & Khazanovich, L. (2017). Permeable pavement in northern North American urban areas: research review and knowledge gaps. *International Journal of Pavement Engineering, 20*, 1–20.
36. Rahman, M. A., Imteaz, M. A., Arulrajah, A., Piratheepan, J., & Disfani, M. M. (2015). Recycled construction and demolition materials in permeable pavement systems: Geotechnical and hydraulic characteristics. *Journal of Cleaner Production, 90*, 183–194.
37. Drake, J., Bradford, A., & Marsalek, J. (2013). Review of environmental performance of permeable pavement systems: State of the knowledge. *Water Quality Research Journal of Canada, 48*(3), 203–222.
38. Kayhanian, M., Weiss, P. T., Gulliver, J. S., & Khazanovich, L. (2015). The application of permeable pavement with emphasis on successful design, water quality benefits, and identification of knowledge and data gaps: A summary report from the National Center for sustainable transportation. Davis, CA, USA
39. Khankhaje, E., Rafieizonooz, M., Salim, M. R., Mirza, J., Salmiati, A., & Hussin, M. W. (2017). Comparing the effects of oil palm kernel shell and cockle shell on properties of pervious concrete pavement. *International Journal of Pavement Research and Technology, 10*(5), 383–392.
40. Çetin, M. (2015). Consideration of permeable pavement in landscape architecture. *Journal of Environmental Protection and Ecology, 16*(1), 385–392.
41. Rizvi, R., Tighe, S., Henderson, V., & Norris, J. (2010). Evaluating the use of recycled concrete aggregate in pervious concrete pavement. *Transportation Research Record: Journal of the Transportation Research Board, 2164*, 132–140.
42. Nishigaki, M. (2000). Producing permeable blocks and pavement bricks from molten slag. *Waste Management, 20*(2–3), 185–192.
43. Lu, G., Liu, P., Wang, Y., Faßbender, S., Wang, D., & Oeser, M. (2019). Development of a sustainable pervious pavement material using recycled ceramic aggregate and bio-based polyurethane binder. *Journal of Cleaner Production, 220*, 1052–1060.
44. Monrose, J., Tota-Maharaj, K., Mwasha, A., & Hills, C. (2019). Effect of carbon-negative aggregates on the strength properties of concrete for permeable pavements. *International Journal of Pavement Engineering, 89*, 1–9.
45. Sañudo-Fontaneda, L. A., Charlesworth, S. M., Castro-Fresno, D., Andres-Valeri, V. C. A., & Rodriguez-Hernandez, J. (2014). Water quality and quantity assessment of pervious pavements performance in experimental car park areas. *Water Science and Technology, 69*(7), 1526–1533.
46. Rodriguez-Hernandez, J., Andrés-Valeri, V. C., Ascorbe-Salcedo, A., & Castro-Fresno, D. (2015). Laboratory study on the stormwater retention and runoff attenuation capacity of four permeable pavements. *Journal of Environmental Engineering, 142*(2), 04015068.
47. Lalla, J. R. F., & Mwasha, A. (2014). Investigating the compressive strengths of Guanapo recycled aggregate concrete as compared to that of its waste material. *West Indian Journal of Engineering, 36*(2), 12–19.
48. Tatsuoka, F., Tomita, Y.-I., Iguchi, Y., & Hirakawa, D. (2013). Strength and stiffness of compacted crushed concrete aggregate. *Soils and Foundations, 53*(6), 835–852.
49. Bentarzi, Y., Terfous, A., Ghenaim, A., Wanko, A., Hlawka, F., & Poulet, J. B. (2013). Hydrodynamic characteristics of a new permeable pavement material produced from recycled concrete and organic matter. *Urban Water Journal, 10*(4), 260–267.
50. Kawalec, J., Kwiecien, S., Pilipenko, A., & Rybak, J. (2017). Application of crushed concrete in geotechnical engineering—Selected issues. *IOP Conference Series: Earth and Environmental Science, 95*, 022057.
51. Cook, D. J. (1983). In R. N. Swamy (Ed.), *Expanded polystyrene concrete* (pp. 41–69). London: Surrey University Press.
52. Mwasha, A., Armstrong-Richardson, A., & Wilson, W. (2013). Management of polystyrene wastes using a supercritical solvent—Propanone. *The Journal of Association of Professional Engineers of Trinidad and Tobago, 41*(1), 23–28.
53. Ahmed Shaikh, F. U., Nath, P., Hosan, A., John, M., & Biswas, W. K. (2019). Sustainability assessment of recycled aggregates concrete mixes containing industrial by-products. *Materials Today Sustainability, 5*, 100013.

54. Azam, A., Gabr, A., Ezzat, H., Arab, M., Alshammari, T. O., Alotaib, E., & Zeiada, W. (2024). Life cycle assessment and pavement performance of recycled aggregates in road construction. *Case Studies in Construction Materials, 20*, e03062.
55. Manjunatha, M., Preethi, S., Malingaraya, A., Mounika, H. G., Niveditha, K. N., & Ravi, K. (2021). Life cycle assessment (LCA) of concrete prepared with sustainable cement-based materials. *Materials Today: Proceedings, 47*(13), 3637–3644.
56. Adhikary, S. K., & Ashish, D. K. (2022). Turning waste expanded polystyrene into lightweight aggregate: Towards sustainable construction industry. *Science of the Total Environment, 837*, 155852.
57. Pratt, C. J. (1990). Permeable pavements for stormwater quality enhancement. In *Engineering foundation conference, Davos Platz, Switzerland*.
58. Pezzaniti, D., Beecham, S., & Kandasamy, J. (2009). Influence of clogging on the effective life of permeable pavements. *Water Management, 162*(3), 211–220.
59. Yong, C. F., McCarthy, D. T., & Deletic, A. (2013). Predicting physical clogging of porous and permeable pavements. *Journal of Hydrology, 481*, 48–55.
60. Nichols, P. W. B., White, R., & Lucke, T. (2015). Do sediment type and test durations affect results of laboratory-based, accelerated testing studies of permeable pavement clogging? *Science of the Total Environment, 511*, 786–791.
61. Ahn, J., Marcaida, A. K., Lee, Y., & Jung, J. (2018). Development of test equipment for evaluating hydraulic conductivity of permeable block pavements. *Sustainability, 10*(7), 2549.
62. ASTM C136/C136M standard test method for sieve analysis of fine and coarse aggregates. ASTM International, West Conshohocken, PA USA (2014).
63. Collins, K. A., & Hunt, W. F. (2008). *Permeable pavement: Research update and design implications*. North Carolina State University.
64. ASTM C127 standard test method for relative density (specific gravity) and absorption of coarse aggregate. ASTM International, West Conshohocken, PA USA (2015).
65. ASTM C29/C29M standard test method for bulk density ("unit weight") and voids in aggregate. ASTM International, West Conshohocken, PA USA (2016).
66. ASTM C131/C131M standard test method for resistance to degradation of small-size coarse aggregate by abrasion and impact in the Los Angeles machine. ASTM International, West Conshohocken, PA USA (2014).
67. BS 812-112. (1990). Testing aggregates. Method for determination of aggregate impact value (AIV). British Standard Institution BSI, London, UK.
68. BS EN 933-3. (2012). Tests for geometrical properties of aggregates. Determination of particle shape. Flakiness index. British Standard Institution BSI, London, UK.
69. BS 1377-3. (2018). Methods of test for soils for civil engineering purposes. Chemical and electro-chemical tests. British Standard Institution BSI, London, UK.
70. Erlingsson, S., & Brencic, M. (2009). A. Dawson. In A. Dawson (Ed.), *Water flow theory for saturated and unsaturated pavement material* (pp. 23–44). Springer.
71. Poon, C., & Chan, D. (2006). Feasible use of recycled concrete aggregates and crushed clay brick as unbound road sub-base. *Construction and Building Materials, 20*(8), 578–585.
72. ASTM D4439 Standard terminology for geosynthetics. ASTM International, West Conshohocken, PA USA (2018).
73. Tota-Maharaj, K., Grabowiecki, P., Akintunde, B., Coupe, S. J. (2012). The performance and effectiveness of geotextiles within permeable pavements for treating concentrated stormwater. In *Sixteenth international water technology conference*, IWTC 16, Istanbul, Turkey.
74. Nnadi, E. O., Coupe, S. J., Sañudo-Fontaneda, L. A., & Rodriguez-Hernandez, J. (2014). An evaluation of enhanced geotextile layer in permeable pavement to improve stormwater infiltration and attenuation. *International Journal of Pavement Engineering, 15*(10), 925–932.
75. Mwasha, A. (2005). *Limited life basal reinforcement for an embankment built on saturated soft clay. Doctoral thesis*. Wolverhampton University.
76. Mwasha, A., & Petersen, A. (2010). Thinking outside the box: The time dependent behaviour of a reinforced embankment on soft soil. *Materials and Design (1980-2015), 31*(5), 2360–2367.
77. Nichols, P. W. B., Lucke, T., & Dierkes, C. (2014). Comparing two methods of determining infiltration rates of permeable interlocking concrete pavers. *Water, 6*(8), 2353–2366.
78. Alsubih, M., Arthur, S., Wright, G., & Allen, D. (2016). Experimental study on the hydrological performance of a permeable pavement. *Urban Water Journal, 14*, 1–8.
79. Nnadi, E. O., Newman, A. P., Coupe, S. J., & Mbanaso, F. U. (2015). Stormwater harvesting for irrigation purposes: An investigation of chemical quality of water recycled in pervious pavement system. *Journal of Environmental Management, 147*, 246–256.
80. Sounthararajah, D. P., Loganathan, P., Kandasamy, J., & Vigneswaran, S. (2017). Removing heavy metals using permeable pavement system with a titanate nano-fibrous adsorbent column as a post treatment. *Chemosphere, 168*, 467–473.
81. Mai, Y., Zhang, M., Chen, W., Chen, X., Huang, G., & Li, D. (2018). Experimental study on the effects of LID measures on the control of rainfall runoff. *Urban Water Journal, 15*(9), 827–836.
82. Monrose, J., & Tota-Maharaj, K. (2018). Technological review of permeable pavement systems for applications in small island developing states. *CLEAN – Soil, Air, Water, 46*(9), 1700168.
83. Erlingsson, S., Baltzer, S., & Baena, J. (2009). J. Bjarnason. In A. Dawson (Ed.), *Measurement techniques for water flow* (pp. 45–67). Springer.
84. Das, B. M. (2010). *Fundamentals of geotechnical engineering* (7th ed., pp. 166–168). Chris Carson.
85. IBM, IBM SPSS statistics for Windows, version 20.02011, IBM Corp, New York, USA.
86. Grontmij A/S PRIMA 100 LWD user manual, Denmark (2012).
87. Hoffmann, O.J.-M., Guzina, B. B., & Drescher, A. (2004). Stiffness estimates using portable deflectometers. *Transportation Research Record: Journal of the Transportation Research Board, 1869*(1), 59–66.
88. Stamp, D. H., & Mooney, M. A. (2013). Influence of lightweight deflectometer characteristics on deflection measurement. *Geotechnical Testing Journal, 36*(2), 216–226.

Kiran Tota-Maharaj - Professor Kiran Tota-Maharaj is a highly regarded academic and engineer holding a professorship at the Royal Agricultural University and a technical director role at the Water Research Centre Ltd (WRc). His expertise spans from environmental engineering, water resources management, sustainable infrastructure, wastewater treatment, and climate change adaptation of water systems.

Sachini Shashiprabha Madushani - Sachini Shashiprabha Madushani is a Civil Engineer pursuing her masters degree in Transportation Engineering. Sachini is a multidisciplinary researcher with research interest on Pavement Engineering, Traffic Engineering, Data science and AI based applications. Sachini is actively contributing to the development of innovative transportation related engineering solutions with publications in leading engineering journals.

John Monrose - Dr. John Monrose is a Civil Engineer and Project Manager at AECOM. He is a Chartered Engineer (CEng) and a Member of the Institution of Civil Engineers (ICE), UK, a Member of the

American Society of Civil Engineers (M. ASCE) and a Registered Engineer (R.Eng) with the Board of Engineering of Trinidad and Tobago (BOETT), West Indies.

Upaka Rathnayake - Professor Upaka Rathnayake is a distinguished academic in the field of civil engineering, currently serving at the Atlantic Technological University (ATU) in Sligo, Ireland. He earned his PhD from the University of Strathclyde, Scotland, and has been active in academia since 2006. His expertise encompasses multiobjective optimization strategies for urban sewer systems, optimal control of urban water systems, soft computing techniques in water resources, and assessing the impact of climate change on water resources.